Available online at www.sciencedirect.com

ScienceDirect

Chinese Journal of Natural Medicines 2018, **16**(11): 0856–0865
doi: 10.3724/SP.J.1009.2018.00856

Chinese Journal of Natural Medicines

Ursane derivatives isolated from leaves of *Hylocereus undatus* inhibit glycation at multiple stages

ROSA MARTHA Pérez-Gutiérrez*, SUSANA GABRIELA Enriquez-Alvirde

Research Laboratory of Natural Products, School of Chemical Engineering and Extractive Industries, National Polytechnic Institute, Av. Instituto Politecnico Nacional S/N, Zacatenco, D.F. CP 07758, Mexico

Available online 20 Nov., 2018

[ABSTRACT] The present study was designed to evaluate the therapeutic potential of bioactive compounds from chloroform extract of the leaves of *Hylocereus undatus* in the formation of advanced glycation end products (AGEs) *in vitro*. Bioactivity-guided fractionation of chloroform extract from *Hylocereus undatus* afforded two novel 12-ursen-type triterpenes, 3*β*, 16*α*, 23-trihydroxy-urs-12-en-28-oic acid (**1**) and 3*β*, 6*β*, 19*α*, 22*α*-tetrahydroxy-urs-12-en-28-oic acid (**2**), as well as four known triterpenes 2*α*, 3*β*, 23-tetrahydroxy-urs-11-en-28-oic acid (**3**), 3*β*-acetoxy-28-hydroxyolean-12-ene (**4**), 3*β*, 16*α*-dihidroxyolean-12-ene (**5**) and 3*β*-acetoxy-olean-12-ene (**6**). Our results revealed that triterpenes **1**–**3** were able to inhibit the formation of AGEs in all tested assays. The data indicated that the triterpenes had inhibitory activity at the múltiple stages of glycation and that there might be a high potential for decreasing protein oxidation and protein glycation that can enhance glycative stress in diabetic complications.

[KEY WORDS] *Hylocereus undatus*; Advanced glycation end product; Triterpenes

[CLC Number] R284.1, R965 **[Document code]** A **[Article ID]** 2095-6975(2018)11-0856-10

Introduction

Advanced glycation end products (AGEs) play an important role in the development of chronic diabetic complications. Diabetes is a disease characterized by chronic hyperglycemia which facilitates nonenzymatic glycation of proteins, producing a partial loss of protein activity [1]. More particularly, the formation of AGEs is divided into three main stages: early, intermediate, and late [2]. In the early stage, various reductive sugars react with the free amino groups of proteins to produce fructosamines, Schiff bases, and Amadori products. In the intermediate stage, Amadori products are transformed into a variety of carbonyl compounds, such as methylglyoxal and glyoxal. In the late stage, irreversible AGEs are formed. Subsequently AGEs induce the formation of reactive oxygen species, generating oxidative stress and vascular inflammation and thus playing an important role in the pathogenesis of vascular complications in diabetes [3]. In diabetic patients, the levels of oxidative stress are much higher than healthy individuals, which is associated with the decrease in the antioxidant enzymes such as glutathione peroxidase, superoxide dismutase, and catalase and increases in protein carbonyls, conjugated diene, and malondialdehyde [4]. In addition, lipid peroxidation and sugar autoxidation are sources of dicarbonyls compounds that are important precursors leading to the formation of AGEs [5].

Due to the evidence about the adverse effects of AGEs on the patients with diabetes, the use of anti-AGEs therapy has thus attracted considerable attention from the researchers in the last decades [6]. Synthetic compounds, such as aminoguanidine (AG), pyridoxamine, LR-90, OPB-9195, ALT-711, and tenilsetam have been developed as antiglycative drugs which have failed in clinical trials in humans due to side effects. Therefore, the investigation of natural antiglycation agents that could ameliorate the diabetic complications with few side effects is very important [7].

Hylocereus undatus (Haworth) Britton & Rose, belongs to the family of the Cactaceae, its fruit is named pitahaya because of the shape of the scales on the fruit skin [8]. The fruits of *H. undatus* are edible and easily marketed in local and regional markets, and its leaves and flowers are traditionally used by the Mayas as a hypoglycaemic, diuretic, and cicatrizing agent [9]. Pharmacological studies on *H. undatus* have shown its beneficial effects on insulin resistance and hepatic steatosis in high-fat-diet-fed mice [10]. Previous studies in our laboratory have revealed wound healing properties of the leaves [11]. In another research, the extracts from *H. undatus* demonstrate

[Received on] 18-June-2018
[Research funding]
[*Corresponding author] Tel: 55-57296000, E-mail: rmpg@prodigy.net.mx
These authors have no conflict of interest to declare.

antioxidant and cytotoxic activities [12]. Phytochemical analysis has shown that flowers are rich in glycosides such as undatusides A–C [13], and flavonoids glucosides [14]. Betacyanin pigments from fruit could be an attractive source of red colorant for food application [15]. Several polysaccharides from *H. undatus* have been purified and identified [16]. In another study, quantification of major flavonoids in flowers of *H. undatus* is carried out using high performance liquid chromatography [17]. In addition, betacyanins from *H. undatus* reduces HFD-induced body weight gain and ameliorates adipose tissue hypertrophy, glucose intolerance, hepatosteatosis, and insulin resistance [18]. Therefore, the aim of the present study was to investigate the effect of triterpenes from leaves of *H. undatus* on the formation of AGEs.

Results

Identification of triterpenes

Compound **1** was obtained as an amorphous white powder, and its molecular formula $C_{30}H_{48}O_5$ was determined by positive high resolution-electrospray ionization mass spectrometry (HR-ESI-MS), which showed a peak at *m/z* 488.3521 indicating 7 degrees of unsaturation, which suggested that it might be a pentacyclic triterpenoid. The IR spectrum of **1** exhibited absorptions from hydroxyl (3462 cm^{-1}), carbonyl (1734 cm^{-1}) and double bond (1638 cm^{-1}) functional groups. Analysis of ^{1}H NMR, ^{13}C NMR, COSY, DEPT, NOESY, and HMBC of **1** suggested 30 carbon signals including the presence of six methyls (δ_C 14.1, 16.3, 20.6, 24.2, 18.4 and 23.1), ten methylenes (including three oxygenated methylene at δ_C 76.8, δ_C 78.0, and δ_C 64.8), six methane (including an olefinic methine δ_C 125.4 to C-12), and eight quaternary carbons (including one olefinic quaternary carbons at δ_C 140.8 (C-13) and a carboxyl carbon at δ_C 179.3 (C-28). The consistent NOESY and HMBC spectral data suggested **1** had the same A/B/C/D/E ring system ursane acid possessing a $\Delta^{12, 13}$. Table 1 summarizes the ^{1}H-, and ^{13}C NMR data, together with HMBC

Table 1 ^{1}H NMR (300 MHz) and ^{13}C NMR (100 MHz) spectroscopic data of compounds 1 and 2 in $CDCl_3$

Position	1		2	
	δ_H	δ_C	δ_H	δ_C
1	*α*: 1.70, 1H, ddd (12.4, 3.1, 3.1) *β*: 0.93, 1H, m	39.4	*α*: 1.73, 1H, ddd (11.4, 3.4, 3.4) *β*: 0.95, 1H, m	38.9
2	*α*: 1.63, 1H, m *β*: 1.56, 1H, m	27.8	*α*: 1.68, 1H, m *β*: 1.65, 1H, m	27.6
3	3.23, 1H, dd (11.6, 5.0)	76.8	3.24, 1H, dd (11.5, 4.6)	77.6
4	-	54.5	-	37.8
5	1.67, m	47.5	1.34, m	57.2
6	*α*: 1.73, 1H, m *β*: 1.36, 1H, m	18.6	4.70, 1H, m	69.3
7	*α*: 1.77, 1H, m *β*: 1.30, 1H, m	29.7	1.96, m	42.2
8	-	38.5	-	38.7
9	1.80, 1H, m	46.1	1.52, 1H, dd (11.0, 6.3)	46.9
10	-	36.0	-	
11	*α*: 2.28, 1H, m *β*: 2.16, 1H, m	24.6	*α*: 2.25, 1H, m *β*: 2.13, 1H, m	24.4
12	5.30, 1H, br, t (3.4)	125.4	5.51, 1H, t (3.3)	128.7
13	-	140.8	-	139.9
14	-	43.6	-	43.2
15	*α*: 1.19, 1H, m *β*: 1.56, 1H, m	35.5	*α*: 1.39, 1H, m *β*: 1.76, 1H, m	27.8
16	3.73, 1H, dd (12.7, 5.3)	76.0	*α*: 2.63, 1H, ddd (133, 4.5, 3.0) *β*: 1.66, 1H, m	25.4
17	-	48.2	-	54.8
18	1.59, m	54.7	3.0, 1H, s	54.7
19	1.30, 1H, m	39.5	-	73.1
20	1.30, 1H, m	39.4	1.77, 1H, m	41.0
21	*α*: 1.13, 1H, m *β*: 1.52, 1H, m	30.7	*α*: 2.47, 1H, q (12.0) *β*: 1.88, 1H, m	36.0
22	*α*: 1.96, 1H, m *β*: 1.75, 1H, m	36.9	4.43, 1H, dd (12.1, 3.6)	74.4
23	*α*: 3.9, 1H, d (10.9) *β*: 3.48, 1H, d (10.9)	66.8	1. 32, 3H, s	24.2
24	0.91, 3H, s	20.1	1. 65, 3H, s	25.6
25	0.98, 3H, s	16.3	1. 67, 3H, s	17.3

Continued

Position	1		2	
	δ_H	δ_C	δ_H	δ_C
26	1.23, 3H, s	20.6	1. 72, 3H, s	19.0
27	1.15, 3H, s	24.2	1.77, 3H, s	25.9
28	-	179.3	-	179.5
29	0.94, 3H, d (10.5)	18.4	1.50, 3H, s	27.5
30	0.92, 3H, d (10.5)	23.1	1.20, 3H, d (6.7)	16.8

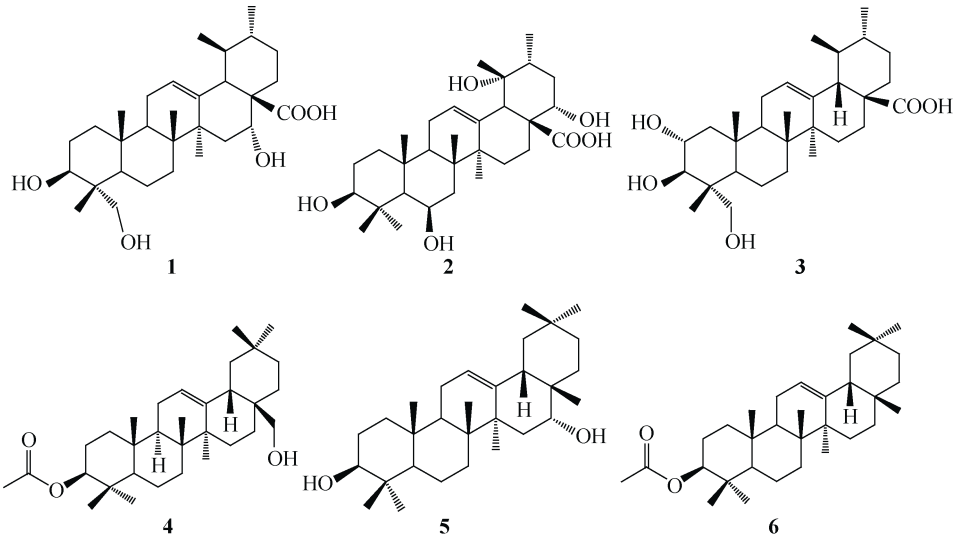

Fig. 1 Chemical structures of triterpenes isolated from *Hylocereus undatus*

correlations, indicating that the structure of **1** was a ursene type triterpenoid [19]. The presence of one hydroxyl group was suggested by the ^{1}H NMR signal at δ_H 3.73 and the ^{13}C NMR signal at δ 76.0 and the position of this hydroxy group was determined to be at C-16 from the ^{1}H–^{1}H (COSY) from H-15 (δ_H 1.19, 1.56) to H-16 (δ_H 3.73), and the HMBC between H-27 (δ_H 1.15) with C-15 (δ_C 35.5), and H-18 (δ_H 1.59) with C-16 (δ_C 76.0) (Fig. 2). The geometry of the hydroxy group was determined be in an *α*-orientation by comparison with ^{13}C NMR data reported for 16-*α* (δ_C ca. 74) and 16-*β* (δ_C ca. 64) hydroxy derivatives of similar compounds [20]. The stereochemistry of 3-OH group was assigned as *β*-equatorial, based on the coupling constant of H-3 (1H, dd, J = 11.6, 5.0 Hz) and NOE correlation between H-3 (δ_H 3.23) and H-23 (δ_H 3.9 and δ_H 3.48) and with δ_H 1.65 (H-24). The HMBC correlations (Fig. 2) between proton signals H-23 (δ_H 3.9, δ_H 3.48), H-24 (δ_H 0.91) and C-3 (δ_C 76.8) confirmed the attachment of the hydroxy group at C-3. The chemical shifts of C-4 (δ_C 54.5) and Me-24 (δ_C 20.1) led to the assignment of the CH_2OH unit at the C-22 position. This was additionally supported by the NOE correlation between H-24 (δ_H 0.91) and H-25 (δ_H 0.98), indicating that the OH group at C-22 has an *α*-orientation [21-23]. In addition, NOESY spectrum displayed correlations between protons H-3/H-5/ H-9/Me-27, supporting that these hidrogens were *α*-orientation. The absolute configuration of compound **1** was considered to be the same with 23-hydroxyursolic acid, based on the similarity of chemical shifts in NMR data [24]. **1** was therefore elucidated as 3*β*, 16*α*, 23-trihydroxy-urs-12-en-28-oic acid (Fig. 1).

Compound **2** was assigned with the molecular formula $C_{30}H_{48}O_6$ as determined by HR-ESI-MS and ^{13}C NMR spectrum, indicating 7 degrees of unsaturation with one carboxyl and a double bond groups, together with the the presence of five tertiary methyls, suggesting the presence of an ursane skeleton. The absorption bands at 1703, 3406, and 1639 cm^{-1} in the IR spectra indicated the presence of carbonyl, hydroxyl and olefin groups, respectively. The ^{1}H- and ^{13}C NMR of **2** was similar to those of 6*β*, 19*α*, 22*α*-trihydroxy-urs-12-en-3-oxo-28-oic acid [21] with the only difference of the OH group at C-6.

The location of the OH group at C-6 was supported by significant HMBC correlations (Fig. 2). Between δ_H 4.70 (H-6) to δ_C 37.8 (C-4), δ_C 57.2 (C-5) and δ_C 38.7 (C-8) which was further supported by NOE correlation between δ_H 4.70 (H-6) and δ_H 1.34 (H-5), indicating the *β*-orientation of the hydroxyl group at C-6. The coupling constant of H-3 (J = 11.5, 4.6 Hz) and NOE correlations between δ_H 3.24 (H-3) and H-23 (δ_H 1. 32), and with δ_H 1.65 (H-24) (Fig. 2) supported the *β*-orientation of the hydroxyl group at C-3. Therefore, **2** was established as 3*β*, 6*β*, 19*α*, 22*α*-tetrahydroxy-urs-12-en-28-oic acid (Fig. 1).

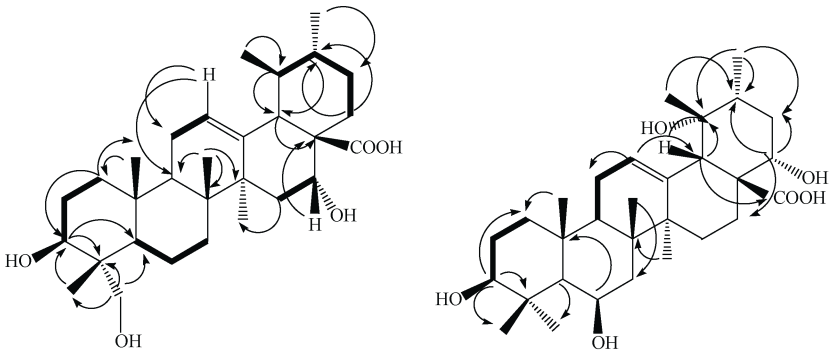

1 **2**

Fig. 2 Correlations HMBC (H-C) and ^{1}H-^{1}H COSY for triterpenes 1 and 2

The structure of the known compounds were characterized by comparisons with the spectroscopic data published in the literature. The known compounds were identified as 2*α*, 3*β*, 13*β*, 23-tetrahydroxy-urs-11-en-28-oic acid (**3**), 3*β*-acetoxy-28-hydroxyolean-12-en (**4**), 3*β*, 16α-dihidroxyolean-12-ene (**5**) and 3*β*-acetoxy-olean-12-ene (**6**) that were previously isolated from *Zizipus jujuba* [23], *Gordonia ceylanica* [25], *Brosimum potabil* [26], and *Trattinnickia burserifolia* [27], respectively.

Effects of triterpenes on the formation of fluorescence AGEs

As shown in Fig. 3, the formation of AGEs was observed by the measurement of an increased fluorescent intensity in glucose-glycated BSA. When BSA was incubated with glucose a significant increase in fluorescent intensity was observed during 4 weeks of the incubation. The results demonstrated that addition of triterpenes **1**, **2**, and **3** (0.5, 1.0, 1.5, and 2.0 mg·mL^{-1} each) significantly reduced the formation of fluorescent AGEs in a concentration-dependent manner (P < 0.05). The results demonstrated that triterpenes **1**, **2** and **3** at different concentrations had significantly (P < 0.05) quenched the fluorescence with values of percentage inhibition of AGE formation ranging from 14.22%–74.29% in glycated BSA, where **3** exhibited maximum inhibition. However, none of triterpenes **4**–**6** affected glycation (data not shown). However, three triterpenes were less potent in the inhibition of AGE formation when compared with AG at the same concentration of 1 mg·mL^{-1}.

Effects of triterpenes on the level of fructosamine

The effects of triterpenes on the level of fructosamine are presented in Table 2. The level of fructosamine in glucose-glycated BSA markedly increased throughout 4 weeks of the experiment. Fructosamine in BSA/glucose system was an early glycation product which was found to be inhibited by **1**, **2** and **3** at concentrations of 5 mmol·L^{-1} with values of 66.2%, 75.4% and 88.7%, respectively, compared with pyridoxamine as positive control (58.3%). Compound **3** exhibited maximum inhibition of the formation of Amadori product.

Effects of MC extract on the formation of Nε-CML

The level of Nε-(carboxymethyl)lysine (Nε-CML), has been used as an indicator for the formation of the non-fluorescent AGEs generated from oxidative breakdown of Amodori product [28]. Glucose-induced glycated BSA exhibited an increase in Nε-CML formation, compared to non-glycated BSA. According to the results, **1**, **2** and **3** at a concentration of 3 mmol·L^{-1} significantly (P < 0.05) inhibited the level of Nε-CML in glycated BSA, with 17.54, 19.48 and 16.17 ng·mL^{-1}, respectively, after 4 weeks of incubation. These results were comparable with those produced by AG (15.25 ng·mL^{-1}). These results of level of Nε-CML are presented in Table 2.

Effects of triterpenes on protein oxidation

In order to determine the protein oxidation, the level of carbonyl content and thiol group formation were used as indicators of protein oxidation during the glycation process. When BSA was incubated with glucose, the level of thiol groups had continuously declined throughout the 4 weeks period. The level of thiol groups after addition of compounds **1**, **2** and **3** indicated protection against thiol oxidation with values ranging from 80.2% to 90.4% (Table 2). The thiol percentages were almost similar to native BSA without glucose, being evident that compounds **1**, **2** and **3** showed strong shielding effects from denaturation. However, AG used as a positive standard, had a low protection of 8.1%.

These findings indicated that the amount of reactive carbonyl in the formation of Girard adduct was decreased in **1**, **2** and **3** treaed groups than that of pyridoxamine (Table 2), which suggested that isolated inhibited AGEs production predominantly by inhibiting dicarbonyl generation. The protein carbonyl compounds were intermediate stage markers found to be inhibited by **1**, **2** and **3** with 21.99%, 19.50% and 23.65%, respectively after 4 weeks of incubation. Adduct in presence of the compound **3** exhibited maximal reduction, compared with AG (22.82%).

Effects of triterpenes on the level of amyloid cross-β structure

Glycation is an important mechanism to generate conformational changes of proteins by increasing the level of amyloid cross *β* structure, which plays an important role in the protein aggregation [28]. The ability of triterpenes to reduce aggregation of glycated albumin was investigated by using two amyloid markers, Thioflavin T (Th. T) and congo Red (Table 2). In glycated albumin samples co-incubated with triterpenes,

similar results exhibited. The presence of **1**, **2,** and **3** demonstrated potent inhibition with both amyloid markers.

Methylglyoxal trapping capacity

As summarized in Fig. 4, Compounds **1**, **2,** and **3** were evaluated for their inhibitory effects on the AGEs formation using BSA–MGO antiglycation model [30]. At the screening dose of 1 mg·mL^{-1}Compound **3** displayed the most potent activity with 72% inhibition, whereas Compounds **1** and **2** had less inhibitory effect with 66% and 58% inhibition, respectively.

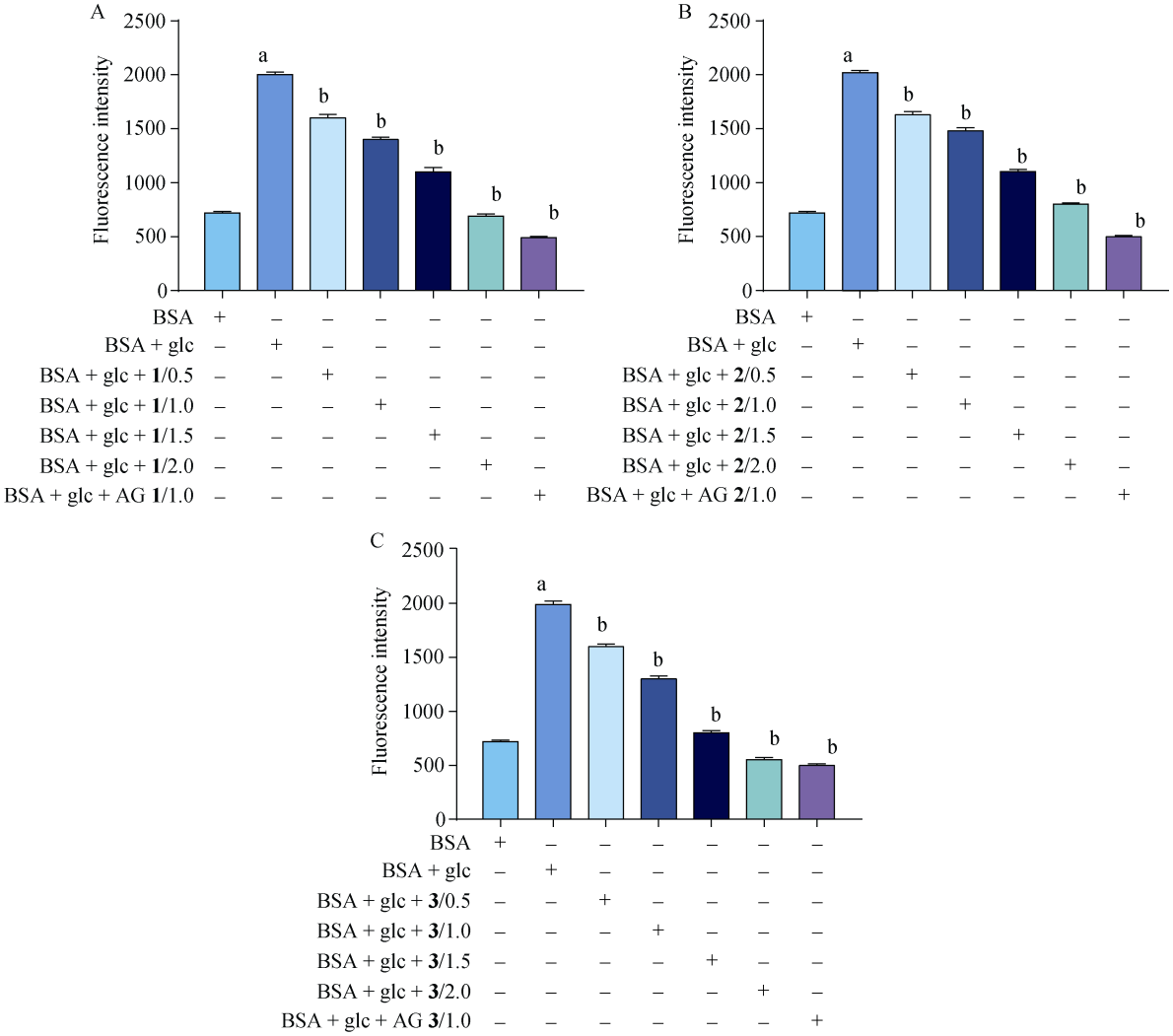

Fig. 3 Effects of 1 (A), 2 (B) and 3 (C) at concentrations of 0.5–2.0 mg·mL^{-1} on formation of fluorescent AGE at 4 weeks of incubation. The results are expressed as means ± SEM (n = 4). $^{a}P < 0.01$, $^{b}P < 0.05$ *vs* BSA/glc

Table 2 Effects of 1, 2 and 3 on the level of Nε-(carboxymethyl)lysine (Nε-CML), carbonyl, thiol content and level of β aggregation in glucose-glycated BSA system (mean ± SEM, n = 4)

Groups	CML (ng·mL^{-1})	Carbonyl content (nmol/mg protein)	Thiol protection (%)	Fructosamines (%)	β aggregation inhibition (%)	
					Congo red	Th.T
BSA/glc	32.50 ± 3.70	2.41 ± 0.08	-	-	-	-
BSA/glc/**1**	17.54 ± 2.65^{a}	1.88 ± 0.27^{a}	86.5 ± 23.19^{a}	66.2	70.2	80.6
BSA/glc/**2**	19.48 ± 2.65^{a}	1.94 ± 0.26^{a}	80.2 ± 12.38^{a}	75.4	69.4	78.4
BSA/glc/**3**	16.17 ± 4.32^{a}	1.84 ± 0.32^{a}	90.4 ± 18.56^{a}	88.7	73.9	84.2
BSA/glc /AG	15.25 ± 2.38^{a}	1.86 ± 0.07^{a}	8.1 ± 1.57	-	-	-
BSA/glc/Pyr	-	-	-	58.3	-	-

$^{a}P < 0.05$ *vs* BSA/glucose; Pyr: Pyridoxamine; Th. T: Thioflavin T

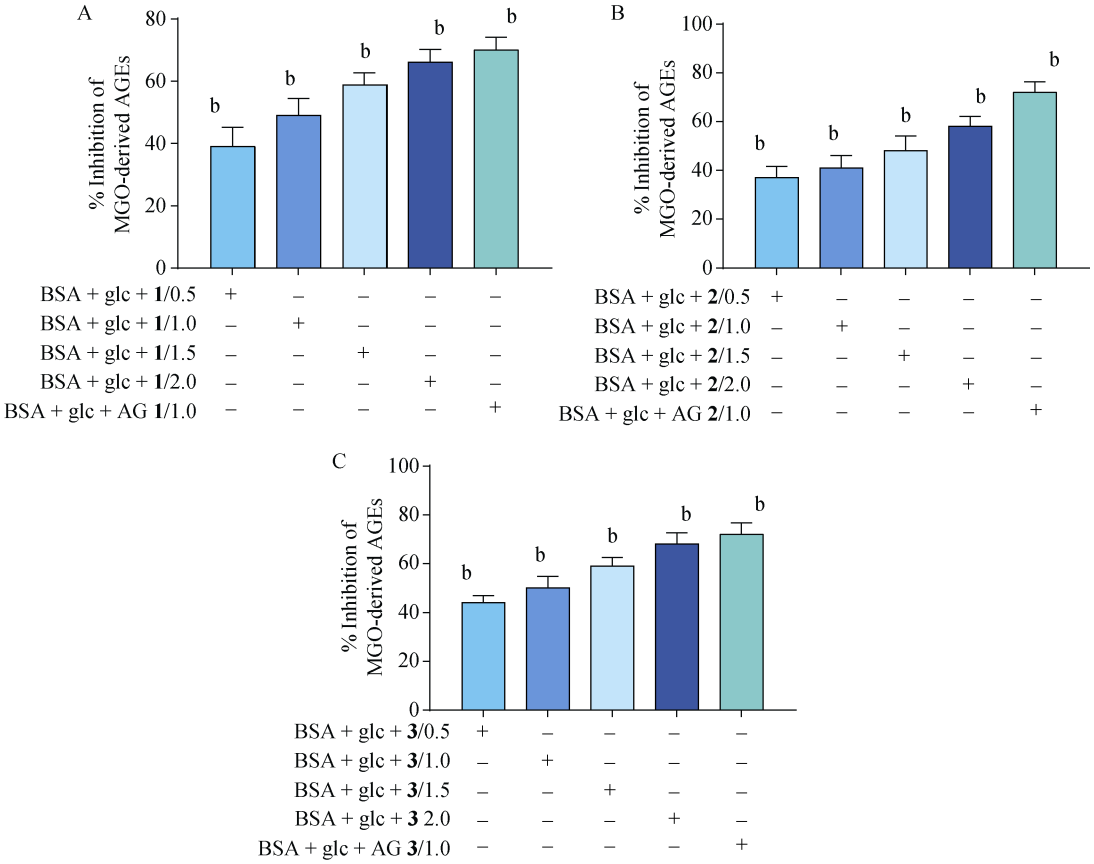

Fig. 4 Percentage of inhibition of triterpenes 1–3 (A–C) at concentrations of 0.5–2.0 mg·mL^{-1} on the formation of MGO-derived AGEs in BSA. data are presented as the mean ± SD, $n = 3$. $^{b}P < 0.05$ *vs* BSA/glc

Structure-activity relationship

The structure-activity relationship analysis suggested that the loss of the carboxyl moiety at C-28 caused a significant loss of activity. No antiglycation activity was observed with Compound **4**–**6** which did not contain a carboxyl group at C-28. These findings also suggested that diol moiety in C-2 and C-3 caused a significant increase in activity, revealing decrease in activity of Compounds **1** and **2**. Additionally, it was subsequently found that the inhibitory effect of Compounds **3** and **1** increased with a hydroxyl group at C-23 or C-24.

Materials and Methods

General experimental procedure

Model infrared (IR) spectra were recorded on a Perkin-Elmer FTIR 1720X spectrometer (Beaconsfield, UK). Proton Nuclear Magnetic Resonance (^{1}H NMR, 300 MHz) and C-13 Nuclear Magnetic Resonance (^{13}C NMR, 75 MHz) spectra were taken on a Bruker DRX-300 NMR spectrometer, (Bruker, Karlsruhe, Germany) and the UXNMR software package was used for NMR experiments. Chemical shifts were reported in δ (ppm), downfield relative to TMS as an internal standard. The NMR experiments were carried out using the conventional pulse sequences as described in the literature [31]. High resolution electron impact mass spectrometry (HR-ESI-MS) was conducted on a JEOL HX 110 mass spectrometer (JEOL, Tokyo, Japan).

Chemicals and reagents

Column chromatography was carried out on Silica gel 60 (230–400 mesh, Merck Co. NJ, USA) and Sephadex LH-20 from Sigma-Aldrich (St. Louis, MO, USA). Precoated TLC silica gel 60 F_{254} aluminum sheets were used (Merck Co. NJ, USA), cloruro de nitroblue tetrazolium (NBT), 1-deoxy-1-morpholino-D-fructose (DMF), bovine serum albumin (BSA), aminoguanidine (AG), 2, 4-dinitrophenylhydrazine (DNPH), and 5, 5′-dithiobis-(2-nitrobenzoic acid) (DTNB) were obtained from Sigma. OxiSelect™ Nε- (carboxymethyl) lysine (CML) ELISA kit was purchased from Cell Biolabs (San Diego, CA, USA). All other chemicals used in the present study were of analytical grade from Fermont (Los Angeles, CA, USA).

Plant materials

Fresh leaves of *Hylocereus undatus* (Cactaceae) were collected in the Oaxaca State. They were verified by the Herbarium of the Metropolitan Autonomous University-Xochimilco. A representative specimen was kept (No. 8967) for further reference.

Isolation of the active constituents of H. undatus

The powdered dried leaves of *H. undatus* (9 kg) were

repeatedly extracted with 40 L of chloroform under reflux for 3 h. The extract was concentrated under *vacuo* to yield a brown residue (600 g). The chloroform extract was subjected to separation on silica gel column (500 g) chromatography eluted with chloroform/acetone 10 : 1 to afford 5 fractions (F1–F5). Each fraction (65 mL) was monitored by thin layer (TLC); fractions with similar TLC patterns were combined. Each fraction was monitored for its anti-glycation effect in BSA/glc system. Subfraction F2 was subjected to silica gel column (1 kg) chromatography using as eluent chloroform/acetone 9 : 0.5 to produce nine subfractions (F2-1 to F2-9). In addition, in the separation of F2-3 fraction was used as eluent chloroform–ethyl acetate–hexane 5 : 1 : 1 to collect eight subfractions (F3-1 to F3-8). Subfraction F3-2 was further separated on a silica gel column using *n*-hexane–ethyl acetate–chloroform 1 : 1 : 5 as the eluent to yield six subfractions (F32-1 to F32-6). Subfraction F32-2 was then filtered three times through a Sephadex LH-20 column eluted with a gradient system of chloroform–methanol (70 : 30 to 0 : 100) to afford 7 fractions (F322-1 to F322-7). F322-5 was separated using a silica gel preparative chromatography and eluted with $CHCl_3$–acetone–CH_2Cl_2 10 : 1 : 2 to give a mixture compounds (F322-1 to F322-4). Subfraction F322-3 was separated using a silica gel preparative chromatography and eluted with petroleum eter–acetone 7 : 3. These procedures yielded pure compounds **1** (79 mg), **2** (68 mg), and **3**(64 mg). The F33-5 mixture was further purified using preparative chromatography eluted with AcOEt–methanol 9 : 1 to yield compounds **4** (36 mg), **5** (63 mg), and **6** (57 mg).

Identification of phytochemical compounds

3*β*, 16*α*, 23-Trihydroxy-urs-12-en-28-oic acid (**1**) was obtained as an amorphous white powder, IR (KBr): 3462 (OH), 1734 (C=O), 1638 (double bond), 1463, 1378, 1259, 1172, 1103 cm^{-1}; HR-ESI-MS *m/z* 488.3513 ($C_{30}H_{48}O_5$, Calcd. 488.3502); for ^1H NMR ($CDCl_3$, 300 MHz) and ^{13}C NMR ($CDCl_3$, 75 MHz) data, see Table 1.

3*β*, 6*β*, 19*α*, 22*α*-tetrahydroxy-urs-12-en-28-oic acid (**2**) was obtained as an amorphous white solid, IR (KBr): 3406 (OH), 1703 (C=O), 1639 (double bond), 1411, 1359, 1259, 1188, 1136 cm^{-1}; HR-ESI-MS *m/z* 504.3428 ($C_{30}H_{48}O_6$, Calcd. 504.3451); for ^1H NMR ($CDCl_3$, 300 MHz) and ^{13}C NMR ($CDCl_3$, 75 MHz) data, see Table 1.

In vitro *glycation of BSA*

Glycated samples were prepared by incubating 10 $mg·mL^{-1}$ of bovine serum albumin (BSA) with glucose (250 $mmol·mL^{-1}$) in 1 mL of phosphate buffered-saline (pH 7.4) containing 0.02% sodium azide (NaN_3) at 37 °C for 4 weeks in the absence or presence of triterpenes (0.5, 1.0, 1.5, 2.0 and $mg·mL^{-1}$) or aminoguanidine (AG, 1.0 $mg·mL^{-1}$). Dimethylsulfoxide (DMSO, 4%) was used as a solvent in this assay [32]. Positive control (BSA + glucose) was maintained under similar conditions and all the incubations were performed in triplicates. The unbound glucose from the all samples was removed by dialysis against the phosphate buffer (200 $mmol·L^{-1}$, pH 7.4). The formation of fluorescent AGEs was measured using a spectrofluorometer detector (BIO-TEK, Synergy HT, USA). The fluorescent intensity was measured at an excitation wavelength of 355 nm and emission wavelength of 450 nm. The percentage of fluorescent AGE formation was calculated as follows:

$$\text{Inhibition of fluorescent AGEs (\%)} = [(Fc - FcB) - (Fs - FsB)/(Fc - FcB)] \times 100$$

where Fc and FCB are the fluorescent intensity of control with glucose and blank of control without glucose, and Fs and FsB are the fluorescent intensity of sample with glucose and blank of sample without glucose.

Subsequently, the antiglycation potential of **1**–**6** was determined by estimation of six parameters from dialysates such as fructosamines, AGEs, Nε-(carboxymethyl) Lysine (CML), protein aggregation, protein carbonyls, and protein thiols.

Formation of fructosamine adduct

The levels of fructosamine adduct was measured using nitro blue tetrazolium (NBT) assay [33]. For this purpose, 10 μL of glycated BSA was incubated with 0.5 $mmol·L^{-1}$ of NBT (90 μL) in 100 $mmol·L^{-1}$ carbonate buffer, pH 10.4 at 37 °C. A positive control in carbonate buffer (pH 10.3) was added to 90 μL of 2.5 $mmol·L^{-1}$ of NBT reagent. After 30 min of incubation at 37 °C the mixture was measured at 590 nm. The level of fructosamine was calculated using the following equation:

$$\text{Inhibitory activity (\%)} = [(A_0 - A_1)/A_0] \times 100$$

where A_0 is the absorbance value of the positive control at 530 nm, and A_1 is absorbance of the glycated albumin samples incubating with triterpenes at 530 nm.

Determination of Nε-(carboxymethyl) lysine (CML)

Nε-(carboxymethyl) lysine (CML) was determined using enzyme linked immunosorbant assay (ELISA) kit (Cell Biolabs, San Diego, CA, USA) according to the manufacturer's protocol. The absorbance of dialysates samples was compared with CML-BSA standard provided in the assay kit.

Determination of protein carbonyl content

The carbonyl group in glycated BSA is a marker for protein oxidative damage, and was estimated in the present study, according to the method of Levine *et al.* [34]. Briefly, 400 μL of 10 $mmol·L^{-1}$ of 2, 4-dinitrophenylhydrazine (DNPH) in 2.5 $mol·L^{-1}$ HCl was reacted with 100 μL of glycated BSA at room temperature for 1 h in the dark. Subsequently, glycated BSA was precipitated by 500 μL of tricholoroacetic acid (TCA), left 5 min on ice and then centrifuged at 10 000 *g* for 10 min at 4 °C. The protein pellet was washed with 500 μL of ethanol–ethyl acetate (1 : 1) mixture three times and resuspended in 250 μL of 6 $mol·L^{-1}$ guanidine hydrochloride. The absorbance was measured at 370 nm. The carbonyl content of each sample was calculated based on the extinction coefficient for DNPH (ε = 22 000 $mol^{-1}cm^{-1}$). The results were expressed as nmol carbonyl per mg protein.

Thiol group estimation

The free thiols in glycated albumin samples were measured according to Ellman's assay using DTNB [35]. Briefly, 70 μL

of glycated BSA were incubated with 5 mmol·L^{-1} of 5, 5′-dithiobis-(2-nitrobenzoic acid) (DTNB) in 0.1 mol·L^{-1} PBS (pH 7.4) at 25 °C for 15 min. The absorbance of samples was measured at 410 nm. The free thiol concentration was measured using a standard curve carried out with standard BSA concentrations (0.8 to 4 mg·L^{-1}, corresponding to 19–96 nmol total thiols). The results were expressed as % protection to protein thiols by comparing with the positive control.

Determination of protein aggregation

Thioflavin T (Th., T) Assay

Amyloid cross *β*-structure, a common marker for protein aggregation was measured using a Thioflavin T assay according to the method of Tupe *et al*. [36]. For this purpose, glycated BSA (10 μL) was added to 100 μL of 64 μmol·L^{-1} of thioflavin T in 0.1 mol·L^{-1} PBS, pH 7.4 and incubated at 25 °C for 1 h. The fluorescence intensity was measured at excitation wavelength of 435 nm and emission wavelength of 485 nm with correction for back ground signals without Th.T. The results were expressed as % inhibition, measured by the following formula:

$$\text{Inhibition (\%)} = [(F_0 - F_1)/F_0] \times 100$$

where F_0 is the florescence of the positive control and F_1 is the florescence of the glycated albumin samples co-incubated with triterpenes.

Binding of Congo red

Amyloid cross β structure was estimated by Congo red assay. Briefly, 500 μL of glycated BSA was incubated with 50 μL of 100 μmol·L^{-1} of Congo red in 10% (*V*/*V*) ethanol/phosphate buffer saline (PBS) for 20 min at 25 °C. Absorbance was recorded at 530 nm [37]. The date were expressed as % inhibition calculated by the following formula:

$$\text{Inhibition (\%)} = [(A_0 - A_1)/A_0] \times 100$$

where A_0 is the absorbance at 530 nm of positive control and A_1 is the absorbance at 530 nm of the glycated albumin samples co-incubated with triterpenes.

Formation of methylglyoxal-derived AGE

In investigation of triterpenes as inhibitors on the middle stage of the glycation of protein, MGO trapping capacity was estimated according to the method described by Peng *et al*. [38]. For this purpose, 0.5 mL of BSA (20 mg·mL^{-1}) was incubated with 0.4 mL of 2.5 mmol·L^{-1} of MGO and 0.5 mL of triterpene (0.5–2.0 mg·mL^{-1}) or AG (1.0 mg·mL^{-1}) as positive control in 0.1 mol·L^{-1} PBS, pH 7.4 at 37 °C for 7 days. After incubation, the fluorescence intensity was measured at the excitation wavelength of 370 nm and an emission wavelength of 420 nm.

$$\text{Inhibition of MGO – derived AGEs (\%)} = (\text{FC} - \text{FCB}) - (\text{FS} - \text{FSB})/(\text{FC} - \text{FCB}) \times 100$$

where FC and FCB are the fluorescent intensity of control with MGO and blank of control without MGO, and FS and FSB are the fluorescent intensity of sample with MGO and blank of sample without MGO.

Statistical Analysis

The data were expressed as means ± standard error of mean (SEM), $n = 3$. The data were analyzed using one way ANOVA followed by Tukey's HSD post hoc test. $P < 0.05$ was considered statistically significant.

Discussion

Repeated chromatography on silica gel and Sephadex LH-20 of the chloroform crude extract led to the isolation of six triterpenes. The structures of isolated compounds were determined by NMR techniques including two-dimensional (2D) as ^{1}H–^{13}C heteronuclear multiple bond coherence (HMBC) and ^{1}H–^{1}H correlation spectroscopy (COSY). Two novel ursane type triterpenes 3*β*, 16*α*, 23-trihydroxy-urs-12-en-28-oic acid (**1**) and 3*β*, 6*β*, 19*α*, 22*α*-tetrahydroxy-urs-12-en-28-oic acid (**2**), as well as four known triterpenes 2*α*, 3*β*, 23-tetrahydroxy-urs-11-en-28-oic acid (**3**), 3*β*-acetoxy-28-hydroxyolean-12-ene (**4**), 3*β*, 16*α*-dihidroxyolean-12-ene (**5**) and 3*β*-acetoxy-olean-12-ene (**6**), were identified in the present study.

We also investigated the chemical and biological effects of triterpenes isolates from *H. undatus* on glycation reactions. The reaction modes of protein glycation at different stages were evaluated. In early stage, defined by the production of Amadori products (fructosamine), middle stage consisting of protein modification by the reactive dicarbonyl MGO and a late stage consisting in the production of AGEs markers such as CML and fluorescent AGEs. Compounds **1**–**3** had inhibitory effects on the early stage of glycation. However, this results showed that the antiglycation actions of triterpenes during the early stage of glycation were not entirely due to the inhibition of Amadori products.

Triterpenes significantly reduced the formation of Nε-CML in glycated BSA with decreases in the formation of AGEs. These results indicated that **1**, **2** and **3** inhibited AGEs production predominantly by inhibiting dicarbonyl generation and fructosamine adduct formation. According to our findings, Compounds **1**, **2**, and **3** may inhibit at multiple stages, being able to be involved in all the three stages.

The albumin in plasma is the major source of thiol groups to form intermolecular aggregates and disulfide bonds. Glycation produces a change in the structure of the protein leading to loss of protein thiol groups, which is reflected in the generation of free radicals [39]. The trapping carbonyls during glycation, the blockage of the carbonyl group in reducing sugars, and breaking the crosslinking structure in the formation AGEs are very important stages in the mechanism of action for antiglycating agents [40]. In addition, triterpenes were able to reduce the contents of protein carbonyl and protected thiol groups from oxidation, indicating their strong reduction potential.

Glycation of albumin induces the generation of amyloid fibrils containing a cross beta structure. Amyloid fibril are able to bind with specific dye such as Congo Red and thioflavin T, which are often used to quantify the level of amyloids in glycated albumin samples. Our findings demonstrated that

triterpenes showed markedly inhibition of amyloid aggregation, supporting their potential to prevent the conformation changes in albumin during glycation.

The formation of AGEs is also produced by MGO which is able to react with lysine residues of glycated BSA to form Nε-CML. The formation of AGEs induced by MGO is through multiple steps. Our results indicated that Compounds **1**, **2**, and **3** suppressed the formation of MGO-AGEs, leading to reduction of the formation of AGEs at the late stage.

Conclusion

In the present study, using different *in vitro* glycation models, we found that three triterpenes isolated from *Hylocereus undatus* had inhibitory activity at multiple stages of glycation, such as Amadori products, AGEs-specific fluorescence, late glycation products, and protein-AGEs crosslinking. In addition, **1**–**3** prevented mainly carbonyl formation, and inhibited the formation of MGO-derived AGEs, oxidative protein damages, and thiol oxidation, which were formed under the glycoxidation process. These results demonstrated that, triterpenes **1**–**3** were capable of suppressing the formation of AGEs and protein oxidation *in vitro*. Thus, these compounds might have potential as functional food to prevent the development of diabetic complications.

References

[1] Yamagishi S, Matsu T. Advanced glycation end products, oxidative stress and diabetic nephropathy [J]. *Oxid Med Cell Longev*, 2014, **3**(2): 101-108.

[2] Baker JR, Metcalf PA, Johnson RN, *et al*. Use of protein-based standardsin automated colorimetric determinations of fructosamine in serum [J]. *Clin Chem*, 1985, **31**(9): 1550-1554.

[3] Goh SY, Cooper ME. The role of advanced glycation end-products in progression and complications of diabetes [J]. *J Clin Endocrinol Metab*, 2008, **93**(4): 1143-11452.

[4] Aramsri M, Weerachat S, Chan CB, *et al*. Isoferulic acid, a new anti-glycation agent, inhibits fructose- and glucose-mediated protein glycation *in vitro* [J]. *Molecules*, 2013, **18**(6): 6439-6454.

[5] Lo CY, Li SM, Tan D, *et al*. Trapping reactions of reactive carbonyl species with tea polyphenols insimulated physiological conditions [J]. *Mol Nutr Food Res*, 2006, **50**(12): 1118-1128.

[6] Nakagawa T, Yokozawa T, Terasawa K, *et al*. Protective activity of green tea against free radical- and glucose-mediated protein damage [J]. *J Agri Food Chem*, 2002, **50**(8): 2418-2422.

[7] Chuang YC, Wu MS, Wu TH, *et al*. Pyridoxamine ameliorates the effects of advanced glycation end products on subtotal nephrectomy induced chronic renal failure rats [J]. *J Funct Foods*, 2012, **4**(3): 679-686.

[8] Argueta AV, Cano LM, Rodarte ME. *Atlas De Las Plantas De La Medicina Tradicional Mexicana* [M]. Instituto nacional indigenista, 1994: 1170-1174.

[9] Bravo JJ. *Las Cactáceas de México* [M]. Mexico-Limusa: Grupo Noriega Editores S.A.de C.V., 1991: 111-113

[10] Song HZ, Zheng ZH, Wu JN, *et al*. White pitaya (*Hylocereus undatus*) juice attenuates insulin resistance and hepatic steatosis in diet-induced obese mice [J]. *PLoS One*, 2016, **11**(2): e0149670.

[11] Perez GRM, Vargas R, Ortiz H. Wound healing properties of *Hylocereus undatus* on diabetic rats [J]. *Phytother Res*, 2015, **19**(8): 665-668.

[12] Ardestani A, Yazdanparast R. *Cyperus rotundus* suppresses AGE formation and protein oxidation in a model of fructose-mediated protein glycoxidation [J]. *Int J Biol Macromol*, 2007, **41**(5): 572-578.

[13] Wu X, Wang Y, Huang XJ, *et al*. Three new glycosides from *Hylocereus undatus* [J]. *J Asian Nat Prod Res*, 2011, **13**(8) 728-733..

[14] Yi Y, Wu X, Wang Y, *et al*. Studies on the flavonoids from the flowers of *Hylocereus undatus* [J]. *J Chin Med Mater*, 2011, **34**(5): 712-716.

[15] Liu. XL, Xu. SY, Wang Z. HPLC/MS analysis of the pigments from red-purple pitaya (*Hylocereus undatus*) [J]. *J Wuxi Univ Light Ind*, 2003, **22**: 62-66.

[16] Xu L, Zhang Y, Wang L. Structure characteristics of a water-soluble polysaccharide purified from dragon fruit (*Hylocereus undatus*) pulp [J]. *Carbohydr Polym,* 2016, **146**: 224-230.

[17] Yi Y, Zhang QW, Li SL, *et al*. Simultaneous quantification of major flavonoids in “Bawanghua”, the edible flower of *Hylocereus undatus* using pressurised liquid extraction and high performance liquid chromatography [J]. *Food Chem*, 2012, **135**(2): 528-533.

[18] Song HZ, Chu Q, Xu DD, *et al*. Purified betacyanins from *Hylocereus undatus* peel ameliorate obesity and insulin resistance in high-fat-diet-fed mice [J]. *J Agric Food Chem*, 2016, **64**(1): 236-244.

[19] Mazumder K, Eric RO, Siwu A, *et al*. Ursolic acidderivatives from Bangladeshi medicinal plant, *Saurauja roxburghii*: Isolation and cytotoxic activity against A431 and C6 glioma cell lines [J]. *Phytochem Lett*, 2011, **4**(3): 287-291.

[20] Ma X, Yang C, Zhang Y. Complete assignments of ^{1}H and ^{13}C NMR spectral data for three polyhydroxylated 12-ursen-type triterpenoids from *Dischidia esquirolii* [J]. *Magn Reson Chem*, 2008, **46**(6): 571-575.

[21] Komoto N, Ichikawa M, Ohta S, *et al*. Murine metabolism and absorption of lancemaside A, an active compound in the roots of *Codonopsis lanceolata* [J]. *J Nat Med*, 2010, **64**(3): 321-329.

[22] Adnyana IK, Tezuka Y, Banskota AH, *et al*. Three new triterpenes from the seeds of *Combretum quadrangulare* and their hepatoprotective activity [J]. *J Nat Prod*, 2001, **64**(3): 360-363.

[23] Qiao A, Wang Y, Xiang L, *et al*. Triterpenoids of sour jujube show pronounced inhibitory effect on human tumorcells and antioxidant activity [J]. *Fitoterapia*, 2014, **98**: 137-142.

[24] Luo Y, Xu QL, Dong LM, *et al*. A new ursane and a new oleanane triterpene acids from the whole plant of *Spermacoce latifolia* [J]. *Phytochem Lett*, 2015, **11**: 127-131.

[25] Herat HM. Athukoralage PS, Jamie JF. Two oleanane triterpenoids from *Gordonia ceylanica* and their conversions to taraxarane triterpenoids [J]. *Phytochemistry*, 2000, **54**(8): 823-827.

[26] Abreu VGDC, Silva MCD, Magalhães RM. Chemical constituents from the stem of *Brosimum potabile* (Moraceae) [J]. *Acta Amazon*, 2010, **40**(4): 711-717.

[27] Lima MP, Campos PA, Macedo ML. Phytochemistry of *Trattinnickia burserifolia*, *T. rhoifolia*, and *Dacryodes hopkinsii*: chemosystematic implications [J]. *J Brazil Chem Soc*, 2004,

15(3): 385-394.

[28] Price DL, Rhett PM, Thorpe SR, *et al*. Chelating activity of advanced glycation end-product inhibitors [J]. *J Biol Chem*, **276**: 48967-48972.

[29] Khan MS, Rabbani N, Tabrez S, *et al*. Glycation induced generation of amyloid fibril structures by glucose metabolites [J]. *Protein Peptide Lett*, 2016, **23**(10): 892-897.

[30] Peng X, Cheng KW, Ma J, et al. Cinnamon bark proanthocyanidinsas reactive carbonyl scavengers to prevent the formation of advanced glycation end products [J]. *J Agric Food Chem,* 2008, **56**(6): 1907-1911.

[31] Poole CP. Electron Spin Resonance: A Comprehensive Trea tise on Experimental Techniques [M]. J. Wiley & Sons, Nueva York, 2ª edición, 1983.

[32] Nisha P, Mini S. *In vitro* antioxidant and antiglycation proper ties of methanol extract and its different solvent fractions of *Musa paradisiaca* L. (cv. nendran) inflorescence. [J]. *Intern J Food Prop*, 2014, **17**(2):399-409.

[33] Tupe RS, Kemse NG, Khaire AA, *et al*. Attenuation of glycation-induced multiple protein modifications by Indian antidiabetic plant extracts [J]. *Pharm Biol*, 2017, **55**(1): 68-75.

[34] Levine RL, Garland D, Oliver CN, *et al*. Determination of carbonyl content in oxidatively modified proteins [J]. *Methods Enzymol*, 1990, **186**(1): 464-478.

[35] Ellman GL. Tissue sulfhydryl groups [J]. *Archives Biophys*, 1959, **82**(1): 70-77.

[36] Tupe R, Agte V. Role of zinc along with ascorbic acid and folicacid during long-term *in vitro* albumin glycation [J]. *Brit Nutrit*, 2010, **103**(3): 370-377.

[37] Klunk WE, Jacob RF, Mason RP. Quantifying amyloid by congo red spectral shift assay [J]. *Methods Enzymol*, 1999, **309**(1): 285-305.

[38] Peng X, Cheng KW, Ma J, *et al*. Cinnamon bark proanthocyanidinsas reactive carbonyl scavengers to prevent the formation of advanced glycation end products [J]. *J Agric Food Chem*, 2008, **56**(6): 1907-1911.

[39] Adisakwattana S, Thilavech T, Chusak C. *Mesona chinensis* Benth extract prevents AGE formation and protein oxidation against fructose-induced protein glycation in vitro [J]. *BMC Complement Altern Med*, 2014, 14: 130-139.

[40] Chiazza F, Cento AS, Collotta D, *et al*. Collino protective effects of pyridoxamine supplementation in the early stages diet-induced kidney dysfunction [J]. *Biomed Res Int*, 2017, **2017**(7): 1-12.

Cite this article as: ROSA MARTHA Pérez-Gutiérrez, SUSANA GABRIELA Enriquez-Alvirde. Ursane derivatives isolated from leaves of *Hylocereus undatus* inhibit glycation at multiple stages [J]. *Chin J Nat Med*, 2018, **16**(11): 856-865.